ACTA UNIVERSITATIS CAROLINAE – GEOLOGICA 2006, 49, pp. 107–117

GROWTH PATTERNS IN ROSTRA OF THE MIDDLE JURASSIC BELEMNITE *MEGATEUTHIS GIGANTEUS*: CONTROLED BY THE MOON?

ELENA DUNCA[1], LARISA DOGUZHAEVA[2], BERND R. SCHÖNE[3] and BAS VAN DE SCHOOTBRUGGE[3]

[1] *Department of Paleozoology, Swedish Museum of Natural History, Stockholm*
elena.dunca@nrm.se
[2] *Palaeontological Institute, Russian Academy of Sciences, Moscow*
ldoguzhaeva@rambler.ru
[3] *Institute for Geology and Paleontology, Increments Research Group, University of Frankfurt a. M.*
B.R.Schoene@em.uni-frankfurt.de, van.de.Schootbrugge@em.uni-frankfurt.de

Abstract: In order to determine the timing of growth of belemnite rostra, we analyzed microgrowth patterns of seven, excellently preserved specimens of *Megateuthis giganteus* (v. Schloth.) from the Middle Jurassic of the Hannover area, Germany. Spectral analysis (single spectrum analysis, continuous wavelet transformation) of microgrowth curves suggests that the microgrowth increments and lines formed on a lunar daily basis. Microincrements are arranged in fortnight bundles of 15. Based on this interpretation, we estimated that the ontogenetic age of the studied specimens (at least the well-preserved visible portions) ranged between one and two years. Furthermore, chemical (energy dispersive spectrometry) and structural (X-ray diffractometry, scanning electron microscopy) analyses and monochromatic cathodoluminescence were employed to study the degree of diagenetic alteration, interpret the original mineralogical composition of the guards and explain the reason for the distinct alternation of dark and light laminae (microgrowth lines or rings). We found that the alternation of dark and light laminae in the rostrum is caused by regular changes in density of calcium carbonate rather variable organic content. Orthorostra were originally composed of low-Mg calcite rather than aragonite. The overall high carbon content (35 to 65% higher amounts than expected for pure calcite) indicates the presence of pristine intra-crystalline (and perhaps inter-crystalline) organic matrix. Despite the overall mint preservation, some portions of the rostra (stained blue by Mutvei's solution) have undergone diagenetic alterations such as cementation and/or recrystallization.

Key words: Belemnites, microstructures, growth patterns, lunar periodicity, Jurassic

INTRODUCTION

Belemnite rostra have been used in numerous studies for the reconstruction of paleoenvironmental conditions (e.g., Urey et al., 1951; Podlaha et al., 1998; Price et al., 2000; Longinelli et al., 2002, 2003; McArthur et al., 2000, 2004; Niebuhr & Joachimski, 2002; Voigt et al., 2003; Florek et al., 2004; Rosales et al., 2004; Wierzbowski 2004; van de Schootbrugge et al., 2005). These studies focused on stable isotopes and trace and minor elements to infer ancient water temperatures, interpret seawater isotopic composition and paleoceanography. Yet, little is known about the structure and the growth periodicity of belemnite rostra. Urey et al. (1951) interpreted the oscillations of oxygen isotopes of the belemnite low-Mg calcite as annual temperature variations and used these cycles to estimate the ontogenetic age of these belemnites (four years of age). However, age determinations based on sclerochronological (growth pattern) studies of belemnite rostra have not been employed.

The rostra of most Jurassic and Cretaceous belemnites have three parts with different structures: (1) the primordial and early juvenile rostrum is considered to be organic-rich and often aragonitic in composition, (2) the orthorostrum is a solid calcitic structure that covers the primordial rostrum and (3) the epirostrum is covering the orthorostrum. Bandel and Spaeth (1988) stated that the epirostrum was originally composed of the aragonite polymorph. The ortho- and epirostrum show concentric laminae interpreted as alternating organic (*laminae obscurae*) and inorganic laminae (*laminae pellucidae*) (Müller-Stoll, 1936; Jeletsky, 1966; Barskov, 1970; Spaeth, 1971; Sælen, 1989). These laminae, also called microgrowth lines or microgrowth rings form a specific microgrowth pattern for each rostrum and are considered to have been formed periodically throughout the entire life-span. Similar microgrowth patterns are found in skeletons of many organisms including bivalve shells (e.g., Berry and Barker, 1968; Clark, 1975, 2005a; Evans, 1972; Richardson et al., 1979; Schöne et al., 2002), corals (e.g., Wells, 1963; Cohen and McConnaughey, 2004), fish otoliths (e.g., Pannella, 1971; Gutiérrez and Morales-Nin, 1986), squid statoliths (e.g., Archipkin and Murzov, 1986; Bettencourt and Guerra, 2001), beak and gladius of octopus (Hernández-Lopez et al., 2001; Perez et al., 1996) and have been interpreted as daily growth periodicities. In these organisms, precipitation of skeletal hard parts is regularly retarded resulting in the formation of distinct growth lines. Such structures might thus be useful in estimating precise ontogenetic ages and adding a time axis to geochemical analyses.

Two major reasons may explain the lack of sclerochronological studies of belemnite guards. Firstly, the poor preservation of most specimens prevents the recognition of

pristine microgrowth structures. Secondly, the lack of appropriate techniques required to visualize internal microgrowth patterns in belemnite rostra over larger portions of the belemnite. Mietchen et al. (2005) used magnetic resonance imaging (MRI) to study pathological deformations of belemnites and to reveal internal growth patterns. However, the resolution of present MRI techniques is insufficient to resolve µm-scale structures. Microgrowth patterns are much better visible in standard petrographic thin-sections viewed under polarized light or gently etched polished thick-sections viewed under reflected light (Mutvei, 1964; Sælen, 1989; O'Neill et al., 2003).

In the present study, we use a new approach to the analysis of microgrowth patterns of belemnite rostra using sclerochronological techniques similar to those applied to bivalve shells (Dunca and Mutvei, 2001; Schöne et al., 2004; Dunca et al., 2005): immersion in Mutvei's solution (Schöne et al., 2005), digital image processing and time-series analyses (Mallat, 1989; Keppenne and Ghil, 1992; Torrence and Compo, 1998). Our aim was to determine whether the microgrowth increments in the rostra of *Megateuthis giganteus* (v. Schloth.) reflect periodicities in the width and density. In order to elucidate the primary cause of the alternation of light and dark laminae we paid special attention to the content of organic matter in the orthorostra. For this purpose, we selected exceptionally well-preserved belemnite rostra with traces of organic matter (Doguzhaeva et al., 2002). Results of the present study will help to better understand life history traits of belemnites and to estimate the timing contained in certain shell portions.

MATERIAL AND METHODS

Seven specimens of *Megateuthis giganteus* (v. Schloth.) from the Middle Jurassic of the Pfullingen, Würtenberg, southern Germany (belonging to the collections of Swedish Museum of Natural History, Stockholm) were chosen for our study. The same specimens were previously used by Doguzhaeva et al. (2002) to describe the general morphology of the pro-ostracum as well as the ultrastructure of the shell wall and the mantle tunic. The maximum diameter of the specimens ranged between 30 and 40 mm.

We prepared median- and cross-sections of the protoconch of all specimens. In order to enhance the visibility of the microgrowth rings, the cross-sections were also made parallel to the c-axes of the calcite prisms and not perpendicularly to the growth axis of the rostrum. The sections were immersed in Mutvei's solution (SCHÖNE et al., 2005) for ca. two hours. This agent is a 1:1 mixture of glutardialdehyde (25%) and acetic acid (1%) to which Alcian blue powder (ca. 5 to 10 g per liter solution) was added. Mutvei's solution is ideal to make fine structural details of biogenic carbonates and phosphates visible in three dimensions (Mutvei, 1979; Dunca and Mutvei, 2001; Schöne et al., 2004; Dunca et al., 2005) and is superior to simple acid treatment (e.g., Sælen, 1989; O'Neill et al., 2003).

Etched sections of the seven rostra were examined using reflected light microscopy (Nikon SMZ 1500; oblique and axial light) as well as scanning electron microscopy (SEM; Hitachi S 4300) at magnifications ranging from ca 20 to 2000 X. The elemental distribution within the rostra was analyzed with energy dispersive spectrometry (EDS) with a spatial resolution of ca 30 µm and detection limit down to ca 1% atomic weight. X-ray diffractometry (XRD) was employed to determine which calcium carbonate polymorph (aragonite, calcite) prevails of the rostra. Possible diagenetic effects were studied with monochromatic cathodoluminesence (CL).

The smallest growth increment (microgrowth increment) in the rostra was defined as the distance between two dark laminae. The width of the microgrowth increments was measured in digital images of the ventral part of the rostra using the Panopea ® image processing software (developed by Peinl and Schöne, University of Frankfurt). Then, the microincrement widths were plotted against microincrement number, linear trends removed and the data were standardized. Spectral analyses of the standardized microincrement time-series included single spectrum analysis (SSA; Keppenne and Ghil, 1992), and continuous wavelet transformation (CWT; Mallat, 1989; Torrence and Compo, 1998). SSA enables decomposition of the chronology into discrete sinusoidal waves and analyses of signal strength (amplitude) through time. Eigenvalues determine the relative proportion of each wavelength in the entire time-series. The focus was on the eight strongest eigenvalues. CWT (here: Morlet function, wavenumber six), however, enables recognition of non-stationary signals, i.e. changes in the amplitude of the dominant (amplitude) wavelengths and frequency evolution of signals through time.

RESULTS

Ultrastructure. Mutvei's solution revealed crisp ultrastructural details in the seven *M. giganteus* rostra. The alternation of the light *laminae pellucidae* and dark *laminae obscurae* seen in the light microscope corresponded to etch-resistant ridges and less etch-resistant depressions seen in SEM (Pl. 1). However, not all the transversal sections were etched homogeneously. Portions of the rostrum were more etch-resistant and more deeply blue stained by the Mutvei's solution (Pl. 2). Neither the *laminae pellucidae* or *laminae obscurae* were interrupted when crossing from blue stained to unstained portions, but they had a different microstructure (smaller crystals with less organized orientation; Pl. 2). Also, the cement that was precipitated in the microcracks of the rostra and the spherulitic structure near the protoconch were strongly bluish stained by the Mutvei's solution (Pl. 2). The blue stained, spherulitic structure within the central part of the juvenile rostrum changed into a colorless prismatic structure after approximately 30 microgrowth increments from the center of the rostrum.

In the colorless portions of the rostra the calcitic prisms were radially arranged and showed a continuous growth toward the outer surface. The prisms were thinner, but not interrupted at the *laminae obscura* (Pl. 3).

All studied rostra exhibited darker regions that had less numerous and narrower laminae. These regions were often stained blue and contained intrusions of spherulitic carbonate.

Microgrowth patterns. We counted up to 567 microincrements in the rostra. The average microincrement width

Table 1. Measurement results.

Specimen no	Museum collection no	Microincrement number	Microincrement width (μm)			Maximal diameter of the rostrum (mm)
			min	max	average	
1	Mo160885	384	4	29	10	30
2	Mo160886	465	4	23	11	42
3	Mo160887	500	6	51	19	34
4	Mo160888	418	3	18	07	37
6	Mo160890	567	2	10	11	44
7	Mo160891	494	4	25	12	43
8	Mo160892	370	4	24	12	31

ranged from 2 μm in specimen no. 6 and 51 μm in specimen no. 3 (Tab. 1). Microgrowth increment measurements revealed up to eight regions with broader microincrements which in turn were separated by regions with narrower microincrements (Pl. 4). Within each specimen, broadest microgrowth increments were found midway between the center and the rim of the cross-section. Growth curves of all studied specimens exhibited distinct periods (eigenvalue pair 7 and 8 in specimens 1–7, eigenvalue pair 3 and 4 in specimen 8) of around 15 ± 2 microincrements (Pl. 5; 6: eigenvalue decomposition and CWTs of decomposed signals). Specimens 1, 3, 4 (eigenvalue pair 3 and 4), 2 (eigenvalue 5) and 7 and 8 (eigenvalue 6) also showed spectral power at frequencies corresponding to approx. 30 ± 2 microincrements. Other spectral power occurred at periods of about 100, 20 and 8 microincrements. In all series, eigenvalues 1 and 2 plotted far away from each other and characterized lower-frequency oscillations. CWTs showed that the 15 ± 2 and the 30 ± 2 microincrement oscillations were nearly stationary in all growth curves. Lower frequency cycles, however, were strongly transient (examples: Pl. 5, A, specimen no. 1 and Pl. 6, C, specimen no. 7).

Chemical analyses. EDS analyses of the seven rostra of *M. giganteus* revealed the following content (in atomic weight %): Ca (ca. 35%), C (ca. 15%) and O (ca. 50%). Trace and minor elements (particularly Mg, Mn, Fe) were lower than the detection limit of the machine. Close to the outer surface of the rostra, EDS showed a higher content of carbon (up to 30%) at the interspaces between the calcium carbonate prisms. The dark and light laminae, however, did not differ in carbon content. CL analyses demonstrated that the portions of the rostrum stained by the Alcian blue have higher luminescence than the unstained portions of the same rostrum.

XDS analysis of specimen no. 7 indicated that the rostra consist of 100% calcite and no aragonite.

DISCUSSION

Ultrastructure and mineralogy. Low amounts of Mg, Mn and Fe within the rostra indicates that the orthorostra of *M. giganteus* were originally composed of (low-Mg) calcite rather that aragonite. This interpretation would be in concert with previous assumptions (Mutvei, 1964; Sælen, 1989; Veizer, 1974) and is supported by the excellent preservation of microgrowth patterns and by the higher carbon content. For pure $CaCO_3$, we would expect 37.7% Ca (atomic weight), 11.3% C and 50.9% O. Our analysis, however, revealed 32.5% higher carbon values than expected in light portions of the rostra and even higher amounts (up to 65% higher than expected) near the outer surface. This observation suggests the presence of original organic matrix in the biominerals and is supported by some previous investigations (Müller-Stoll, 1936; Jeletzky, 1966; Barskov, 1970; Spaeth, 1971; Sælen, 1989).

Preservation of pristine organic matter is not unusual in well-preserved fossil material (Clark, 1999), especially within the crystallites (intra-crystalline organic matrix; Clark, 2005b). Apparently, the dense skeleton of the belemnite rostrum prevented extensive diagenetic alteration, except for portions near the periphery of rostra, within microcracks and in the youngest parts (center) of the rostra. We observed patchy recrystallization through the use of monochromatic CL and immersion in Mutvei's solution. Our findings confirm previous observations on low diagenetic alteration of belemnites (e.g. Podlaha et al., 1998; O'Neill et al., 2003; Rosales et al., 2004).

There is no evidence that organic laminae alternate with inorganic laminae as previously stated (Müller-Stoll, 1936; Jeletsky, 1966; Barskov, 1970; Spaeth, 1971; Sælen, 1989). We did not find a difference in carbon content of dark and light laminae. Rather, the organic material seems to be homogeneously distributed within the rostrum (except for C-enriched outer rim portions), while the alternating lightness of the laminae seems to be the result of different crystal size and density.

Timing of growth of the belemnite guard; microgrowth patterns. Spectral analyses of the microgrowth patterns suggest that the formation of the belemnite guards of *M. giganteus* was controlled by lunar cycles. In all microgrowth increment time-series of *M. giganteus*, sinusoidal components reflecting bundles of 15 and 30 microincrements were among the eight most prominent signals. We assume that these cycles are indicative of fortnight periods of shell formation. Today, however, one fortnight period is slightly shorter and comprises only 13.5 to 14.5 lunar days (perigee and apogee fortnight periods, respectively). Yet, according to astronomical calculations and sclerochronolgical analyses of other Jurassic biogenic skeletons, days in the Jurassic were shorter, because the rotation of the earth around its own axis was faster and the distance between earth and moon closer than today (e.g., Rosenberg, 1977). During the Jurassic, each fortnight period was about one day longer than today. This finding adds support to our hypothesis that the 15 and 30 microincrement bundles reflect fortnight periods and that each microincrement was formed during one lunar day. But can the microincrements

also represent semi-diurnal cycles? This seems unlikely because the 15 microincrement cycle would be much weaker or absent from the chronology. Components of the time-series with lower frequency can be attributed to harmonics of these fortnight periods or were strongly transient indicating growth trends rather than cycles. The hypothesis of a tide-controlled growth of the belemnite guard was also previously suggested by Anisimov et al. (1984), based on optical heterogeneity of ortorostra sections.

Circadian (ca. 24hr period) and circalunidian (two circadian clocks linked in antiphase, hence 12.4 hr intervals, intertidal organisms; term coined by Palmer et al., 1994) periods were observed in a variety of living organisms including humans (sleeping cycle), bivalves (Richardson et al., 1980; Kim et al., 1999), crabs (Palmer et al., 1994) and coleoid cephalopods (Kristensen, 1980; Radtke, 1985). Circadian or circalunidian periodicity of shell growth was also observed in several ammonoid genera (Doguzhaeva, 1982, 1984, 1986, 1990; Checa, 1987).

Laptikhovsky (2002) observed diurnal feeding rhythms in the short-finned squid *Illex argentinus* off the Falkland Islands. Perhaps, similar causes can be assumed for the rhythms retrieved from the belemnite rostra. Biological clocks help organisms to anticipate changes of the environment such as changes of the food supply, light availability etc. (Pittendrigh, 1979; Rensing et al., 2001). Circadian biological clocks are genetically determined and are entrained and constantly reset by environmental pacemakers (Young and Kay, 2001).

Gravitational forces of the moon and sun exert a major control on marine ecosystems (Palmer, 1996). For example, spawning of corals and many other organisms is induced by the tides (e.g., McGuire, 1998). Even deep sea environments are affected by the tidal bulges. Current velocity in deep sea environments varies diurnally and on a fortnightly basis. Near hydrothermal vents, these currents can significantly influence the temperature regime (Johnson et al., 1994) and hence the biological productivity of organisms that directly (chemosymbionts) or indirectly (organisms with chemosymbionts) depend on hydrothermal effluents (Schöne and Giere, 2005).

If our hypothesis on the timing of growth of the rostra is true, the belemnites of our study formed during a period of about one or two years. Such age estimates closely match those of modern cephalopods (e.g. Jackson, 1998).

CONCLUSIONS

(1) Guards of *M. giganteus* formed with lunar daily periodicity. Lunar daily microgrowth patterns were revealed by immersion in Mutvei's solution and can be used to estimate the ontogenetic age of the belemnite and add a precise time axis to geochemical data obtained from the rostra.

(2) The ontogenetic ages of the studied specimens of *M. giganteus* ranged between one to two years.

(3) Orthorostra of *M. giganteus* were originally composed of (low-Mg) calcite.

(4) Carbon is enriched in the rostra by 35 to 65% possibly reflecting the preservation of pristine intra- and intercrystalline organic matrix.

(5) There is no evidence that organic-rich laminae (microgrowth lines) alternate with inorganic laminae (microgrowth increments). The difference between microincrements and –lines seems to be the result of differences in crystal size and orientation.

(6) Despite the overall excellent preservation, EDS, CL and XDS analyses demonstrate that non-homogenous diagenetic alteration occurred (radial microcracks, center of the guards, outer rim).

REFERENCES

Anisimov Y. A., Kalikov V. N., Molin V. A., 1984: Study of the belemnite growth rings with the purpose of determination of Jurassic geochronometry, in: Bogdanov N. A. (ed.), 27th Geological Congress, 4–14 August 1984, Moscow, Abstracts Vol. 1, Sections 01–03, Publishing house "Nauka", Moscow, pp. 235–237.

Arkhipkin A. I., Murzov S. A., 1986: The age and growth periodicity in squid *Dosidicus gigas* (Ommastrephidae). Recourses and perspectives in use of squids in Oceans. Moscow, VNIRO, pp. 107–123. [In Russian]

Bandel K., Spaeth Ch., 1988: Structural Differences in the Ontogeny of some Belemnite Rostra, in: Wiedman J., Kullman J., (eds.), Cephalopods – Present and Past. Schweizerbart'sche Verlagsbuchhandlung, Stuttgart, pp. 247–271.

Barskov I. S., 1970: Structure of belemnitid rostrum. Paleont. J. 4: 110–112.

Berry W. B. N., Barker R. M., 1968: Fossil bivalve shells indicate longer month and year in cretaceous than present. Nature 217: 938–939.

Bettencourt V., Guerra A., 2001: Age studies based on daily growth increments in statoliths and growth lamellae in cuttlebone of cultured *Sepia officinalis*. Mar. Biol. 139: 327–334.

Checa A., 1987: Morphogenesis in ammonites – differences linked to growth patterns. Lethaia 20 (2): 141–148.

Clark G. R., 1975: Periodic growth and biological rhythms in experimentally grown Bivalves, in: Rosenberg G. D., Runcorn S. K. (eds.), Growth Rhythms and the History of the Earth's Rotation. J. Wiley and Sons, New York, pp. 103–117.

Clark G. R., 1999: Organic matrix taphonomy in some molluscan shell microstructures. Palaeogeogr., Palaeocl., Palaeoecol. 149: 305–312.

Clark G. R., 2005a: Daily growth lines in some living Pectens (Mollusca: Bivalvia), and some applications in a fossil relative: Time and tide will tell. Palaeogeogr., Palaeocl., Palaeoecol. 228: 26–42.

Clark G. R., 2005b: Organic matrix in the porifera and cnidaria: déjà vu through a temporal telescope. Geological Society of America Abstracts with Programs 37: 366.

Cohen A. L., McConnaughy T. A., 2003: Geochemical perspectives on coral mineralization. Rev. Mineral. Geochem. 54: 151–187.

Doguzhaeva L. A., 1982: Rhythms of ammonoid shell secretion. Lethaia 15: 385–394.

Doguzhaeva L. A., 1984: Periodicity in ammonoid shell growth and geochronometry, in: Bogdanov N. A., (ed.), 27 Geological Congress, August 4–14 1984, Moscow, Abstracts Vol. 1, Sections 01–03, Publishing house "Nauka", Moscow: pp. 253–254.

Doguzhaeva L. A., 1986: How long did ammonites live. Science in the USSR 3: 113–117.

Doguzhaeva L. A., 1990: The growth analyses in ammonoid shell, in: Shevyrev A. A., Shimanskiy V. N., (eds.), Fossil cephalopods. Evolution and system of different taxa. Trudy of Palaeontological Inst., USSR Acad. Sci. 243, 15–28.

Doguzhaeva L., Mutvei H., Donovan D. T., 2002: Pro-ostracum, Muscular Mantle and Conotheca in the Middle Jurassic Belemnite *Megateuthis*. Cephalopods – Present and Past. Abh. Geol. Bund. 57: 321–339.

Dunca E., Mutvei H., 2001: Comparison of microgrowth pattern in *Margaritifera margaritifera* shells from south and north Sweden. Am. Malacol. Bull. 16: 239–250.

Dunca E., Mutvei H., Schöne B. R., 2005: Freshwater bivalves tell of past climates: But how clearly do shells from polluted rivers speak? Palaeogeogr., Palaeocl., Palaeoecol. 228: 43–57.

Evans J. W., 1972: Tidal growth increments in the cockle Clinocardium nuttalli: Sci. 176: 416–417.

Florek M., Youn H. S., Ro C.-U., Wierzbowski H., Osán J., Kazimierczak W., Kuczumow A., 2004: Investigation of chemical composition of belemnite rostra by synchrotron-based X-ray microfluorescence and diffraction and electron microprobe. J. of Alloys and Comp. 362: 99–106.

Gutiérrez E., Morales-Nin B., 1986: Time series analysis of daily growth in *Dicentrarchus labrax* L. otoliths. J. Exp. Mar. biol. Ecol. 103: 163–179.

Hernández-López J. L., Castro-Hernández J. J., Hernández-García V., 2001: Age determined from the daily deposition of concentric rings on common octopus (*Octopus vulgaris*) beaks. Fish. Bull. 99: 679–684.

Jackson G. D., 1998: Research into the life history of *Loglio opalescens*: where to from here? CalCOFI Rep. 39: 101–107.

Jeletzky J. A., 1966: Comparative morphology, phylogeny and classification of fossil Coleoidea, Mollusca. Paleont. Contr. Univ. Kans. 7: 162.

Johnson K. S., Childress J. J., Beehler C. L., Sakamoto C. M., 1994: Biogeochemistry of hydrothermal vent mussel communities: the deep-sea analogue to the intertidal zone. Deep-Sea Res., Part I 41: pp. 993–1011.

Keppenne C. L., Ghil M., 1992: Adaptive filtering and prediction of the Southern Oscillation Index. J. Geophys. Res. 97: 20449–20454.

Kim W. S., Huh H. T., Lee J.-H., Rumohr H., Koh C. H., 1999: Endogenous circatidal rhythm in the Manila clam *Ruditapes philippinarum* (Bivalvia: Veneridae). Mar. Biol. 134: 107–112.

Kristensen T. K., 1980: Periodical growth rings in cephalopod statoliths. Dana 1: 39–51.

Lapitkhovsky V., 2002: Diurnal feeding rhythm in the short-fin quid *Illex argentinus* (Cephalopoda: Ommastrephidae) in the Falkland waters. Fisch. Res. 1373: 1–5.

Longinelli A., Iacumin P., Ramigni M., 2002: $\partial^{18}O$ of carbonate, quartz and phosphate from belemnite guards: implications for the isotopic record of old fossils and the isotopic composition of ancient seawater. Earth Planet. Sci. Lett. 203: 445–459.

Longinelli A., Wierzbowski H., Di Matteo A., 2002: $\partial^{18}O$ (PO) and $\partial^{18}O$ (PO) from belemnite guards from Eastern Europe: implications for palaeoceanographic reconstructions and for the preservation of pristine isotopic values. Earth Planet. Sci. Lett. 209: 337–350.

Mallat S., 1989: A theory for multiresolution signal decomposition: the wavelet representation. IEEE Pattern Analysis and Machine Intelligence 11: pp. 674–693.

McArthur J. M., Donovan D. T., Thirlwall M. F., Fouke B. W., Mattey D., 2000: Strontium isotope profile of the early Toarcian (Jurassic) oceanic anoxic event, the duration of ammonite biozones, and belemnite palaeotemperatures. Earth Planet. Sci. Lett. 179: 269–285.

McArthur J. M., Mutterlose J., Price G. D., Rawson P. F., Ruffell A., Thirlwall M. F., 2004: Belemnites of Valanginian, Hauterivian and Barremian age: Sr-isotope stratigraphy, composition ($^{87}Sr/^{86}Sr$, $\partial^{13}C$, $\partial^{18}O$, Na, Sr, Mg), and palaeo-oceanography. Palaeogeogr., Palaeocl., Palaeoecol. 202: 253–272.

McGuire M. P., 1998: Timing of larval release by *Porites astreoides* in the northern Florida Keys, Coral Reefs 17: 369–375.

Mietchen D., Keupp H., Manz B., Volke F., 2005: Non-invasive diagnostics in pathological fossils by magnetic resonance imaging. Biogeosci. Discuss. 2: 239–260.

Müller-Stoll H., 1936: Beiträge zur Anatomie der Belemnoidea. Nova Acta Leopoldina, new series 4: 159–226.

Mutvei H., 1979: On the internal structures of the nacreous tablets in molluscan shells. Scan. Electron. Microsc. 2: 457–462.

Mutvei H., 1964: Remarks on the anatomy of recent and fossil Cephalopoda with description of the minute shell structure of belemnoids. Acta Universitatis Stockholmiensis, Stockholm Contrib. Geol. 11: 79–102.

Niebuhr B., Joachimski M. M., 2002: Stable isotope and trace element geochemistry of Upper Cretaceous carbonates and belemnite rostra (Middle Campanian, north Germany). Geobios 35: 51–64.

O'Neill B. R., Manger W. L., Hays P. D., 2003: Growth and diagenesis of Middle Jurassic belemnite rostra from northeastern Utah: insights using cathodoluminescence. Berl. Paläobiol. Abh. 3: 241–251.

Palmer J. D., 1996: Time, tide and living clocks of marine organisms. Am. Scient. 84: 570–578.

Palmer J. D., Williams B. G., Dowse H. B., 1994: The statistical analysis of tidal rhythms: tests of the relative effectiveness of five methods using model simulations and actual data. Mar. Beh. and Physiol. 24: 165–182.

Pannella G., 1971: Fish otoliths: daily growth layers and periodical patterns. Sci. 173: 1124–1127.

Perez J. A. A., O'Dor R. K., Beck P., Dawe E. G., 1996: Evaluation of gladius dorsal surface structure for age and growth studies of the short-finned squid, *Illex illecebrosus* (Teuthoidea: Ommastrephidae). Can. J. Fish. Aquat. Sci. 53: 2837–2846.

Pittendrigh C. S., 1979: Some functional aspects of circadian pacemakers, in: Suda M., Hayaishi O., Nakagawa H. (eds.), Biological Rhythms and Their Central Mechanism. Elsevier / North-Holland Biomedical Press, Amsterdam, Netherlands, pp. 3–12.

Podlaha O. G., Mutterlose J., Veizer J., 1998: Preservation of $\partial^{18}O$ and $\partial^{13}C$ in belemnite rostra from the Jurassic / Early Cretaceous successions. Am. J. Sci. 298: 324–347.

Price G. D., Ruffell A. H., Jones C. E., Kalin R. M., Mutterlose J., 2000: Isotopic evidence for temperature variation during the early Cretaceous (late Ryazanian–mid-Hauterivian). J. Geol. Soc., London 157: 335–343.

Radtke R. L., 1985: Information incorporated in cephalopod statoliths, in: Wiedmann J., Kullmann J., (eds.), 2nd Intern. Cephalopods Symp. "Cephalopods: Present and Past", Abstracts, pp. 99.

Rensing L., Meyer-Grahle U., Ruoff P., 2001: Biological timing and the clock metaphor: oscillatory and hourglass mechanisms. Chronobiol. Intern. 18: 329–369.

Richardson C. A., Crisp D. J., Runham N. W., 1979: Tidally deposited growth bands in the shell of the common cockle *Cerastoderma edule* (L.). Malacol. 18: 277–290.

Richardson C. A., Crisp D. J., Runham N. W., 1980: An endogenous rhythm in shell deposition in *Cerastoderma edule*. J. Mar. Biol. Ass. U. K. 60: 991–1004.

Rosales I., Robles S., Quesada S., 2004: Elemental and oxygen isotope composition of early Jurassic belemnites: salinity vs. temperature signals. J. Sed. Res. 74: 342–354.

Rosenberg G. D., 1977: The development of a chronobiologic time scale. J. interdiscipl. Cycle Res. 8: 211–214.

Sælen G., 1989: Diagenesis and construction of the belemnite rostrum. Palaeont. 32 (4): 765–798.

Schöne B. R., Giere O., 2005: Growth pattern and shell isotope ratios of the deep-sea hydrothermal vent bivalve mollusk *Bathy-*

modiolus brevior from the North Fiji Basin, Pacific Ocean. Deep-Sea Res. I, 52: 947–962.

Schöne B. R., Dunca E., Fiebig, J., Pfeiffer M., 2005: Mutvei's solution: an ideal agent for resolving microgrowth structures of biogenic carbonates. Palaeogeogr., Palaeocl., Palaeoecol. 228: 149–166.

Schöne B. R., Dunca E., Mutvei H., Norlund U., 2004: A 217-year record of summer air temperature reconstructed from freshwater pearl mussels (*M. margaritifera*, Sweden). Quatern. Sci. Rev. 23: 1803–1816, 2057.

Schöne B. R., Lega J., Flessa K. W., Goodwin D. H., Dettman D. L., 2002: Reconstructing daily temperatures from growth rates of the intertidal bivalve mollusk *Chione cortezi* (northern Gulf of California, Mexico). Palaeogeogr., Palaeocl., Palaeoecol. 184: 131–146.

Spaeth C., 1971: Untersuchungen an belemniten des Formenkreises um *Neohibolites minimus* (Miller 1826) aus dem Mittel – und Ober-Alb Nordwestdeutschlands. Geol. Jb. 100: 127.

Torrence C., Compo G. P., 1998: A practical guide to wavelet analysis. Bull. Am. Meteo. Soc. 79: 61–78.

Urey H. C., Lowenstam H. A., Epstein S., McKinney C. R., 1951: Measurement of paleotemperatures and temperatures of the upper Cretaceous of England, Denmark, and the southeastern United States. Bull. Geo. Soc. Am. 62: 399–416.

van de Schootbrugge B., McArthur J. M., Bailey T. R., Rosenthal Y., Wright J. D., Miller K. G., 2005: Toarcian oceanic anoxic event: An assessment of global causes using belemnite C isotope records. Paleoceanogr. 20: doi: 10.1029/2004PA001102.

Veizer J., 1974: Chemical diagenesis of belemnite shells and possible consequences for paleotemperature determinations. N. Jb. Geol. Paläont. Abh. 147: 91–111.

Voigt S., Wilmsen M., Mortimore R. N., Voigt T., 2003: Cenomanian palaeotemperatures derived from the oxygen isotopic composition of brachiopods and belemnites: evaluation of Cretaceous palaeotemperature proxies. Int. J. Earth Sci. 92: 285–299.

Wells J. W., 1963: Coral growth and geochronometry. Nature 197: 948–50.

Wierzbowski H., 2003: Carbon and oxygen isotope composition of Oxfordian-Early Kimmeridgian belemnite rostra: palaeoenvironmental implications for Late Jurassic seas. Palaeogeogr., Palaeocl., Palaeoecol. 203: 153–168.

Young M. W., Kay S. A., 2001: Time zones: a comparative genetics of circadian clocks. Nature Reviews Genetics 2: 702–715.

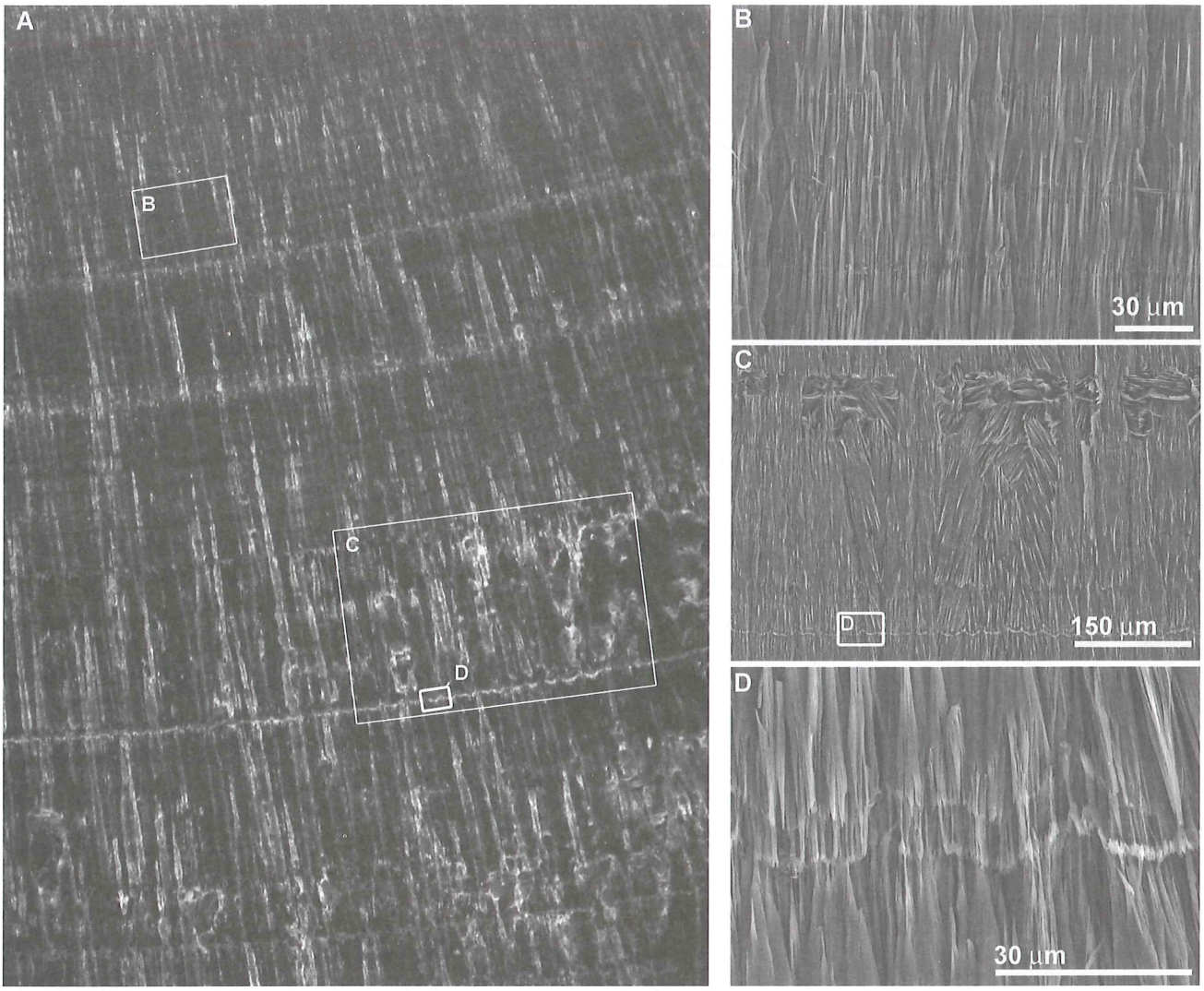

Plate 1. A–D. Thin section of the rostrum of *Megateuthis,* specimen 1, etched with Mutvei's solution. A. The section viewed under a reflective light stereomicroscope with axial light. B, C and D. Portions of the same rostrum viewed in a scanning electron microscope (SEM). The alternation of the light lamina and dark lamina (seen in light microscope) corresponds to ridges and depressions (seen in SEM). The light lamina (ridges) are more etch-resistant than the dark lamina (depressions).

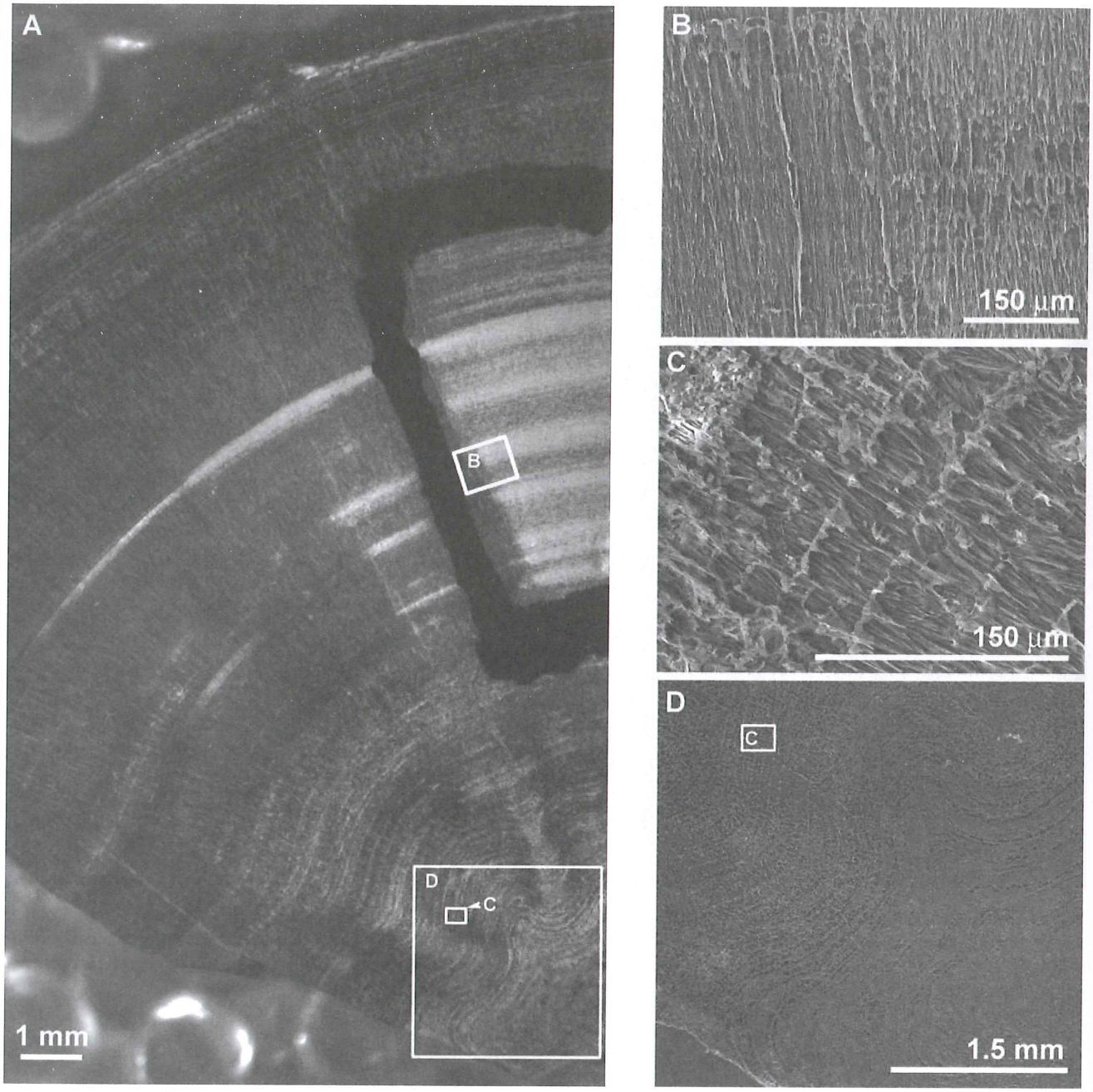

Plate 2. A–D. Portions of the rostrum (specimen 1) stained by Alcian blue are more etch-resistant (even the cement within the cracks) than the colourless portions. B. The growth rings are not interrupted when crossing from blue stained to colourless portions but they have different microstructure. C. The spherulitic microsturcture of the juvenile rostrum is strongly stained by the Mutvei's solution and is more resistant to etching. D. Overview of the central part of the rostrum seen in SEM showing nonhomogenous etching.

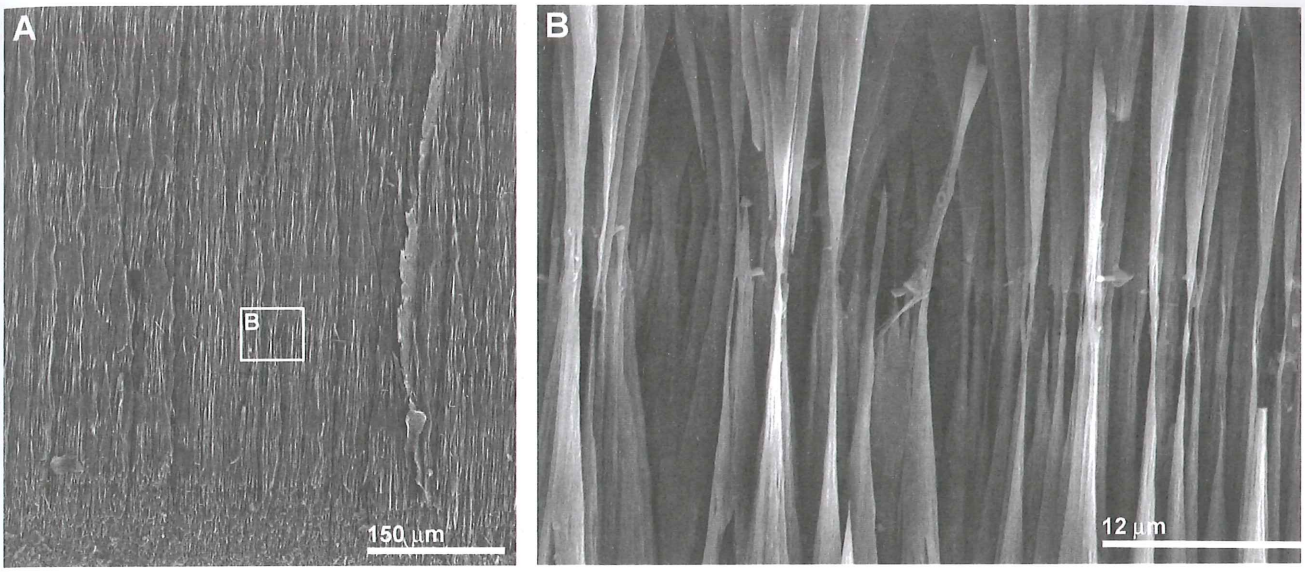

Plate 3. A–B. SEM picture of an unstained portion of the belemnite rostrum, specimen 3, showing that the calcite prisms grow radially and that their growth is not interrupted by dark lamina. B. Detail of a dark laminae that shows the continuous growth of the calcite prisms.

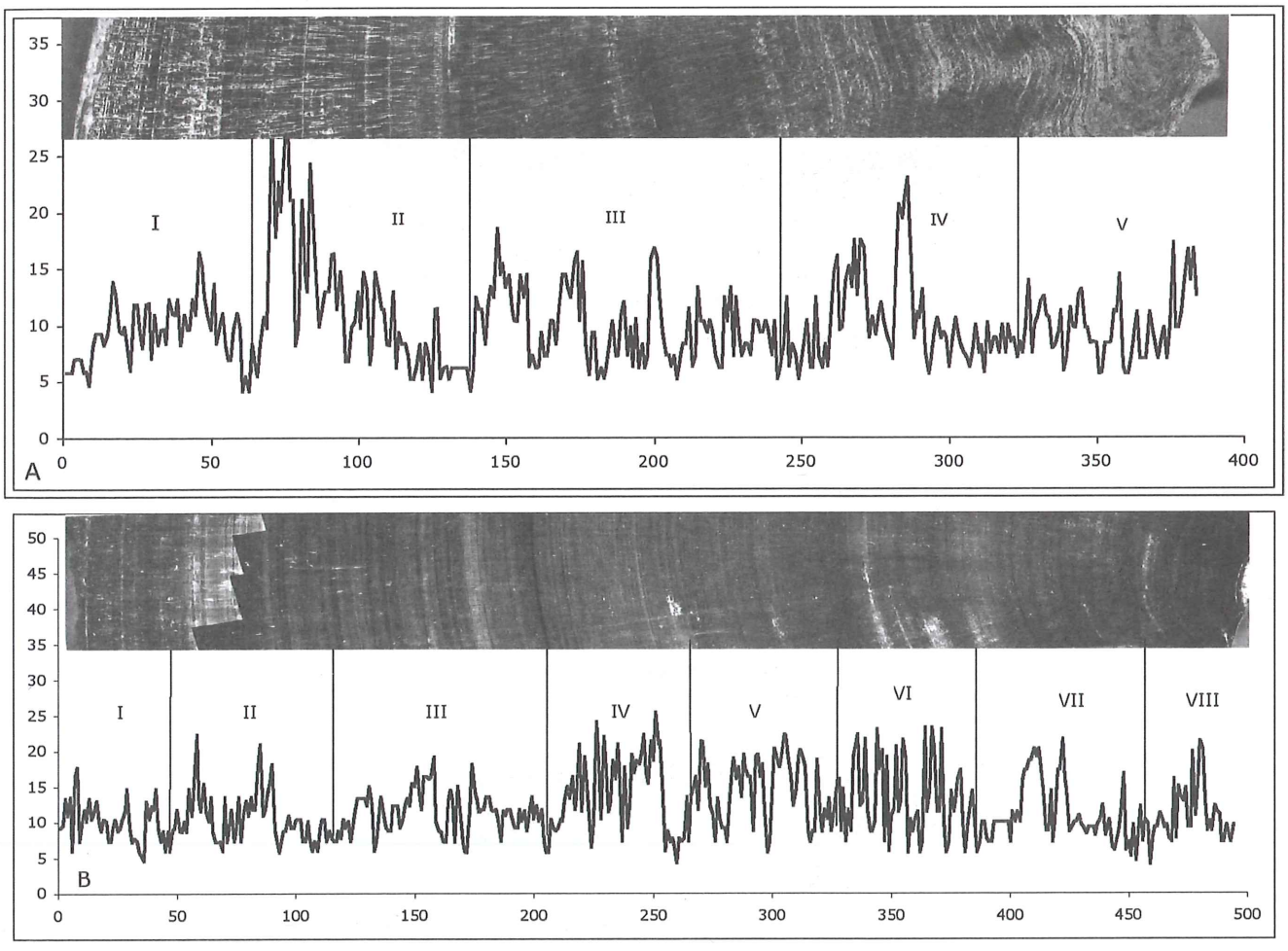

Plate 4. A–B. Growth measurements of two *Megateuthis* rostra: A. specimen no 1 and B. specimen no 7. I–VIII correspond to regions with higher growth rate separated by regions with lower growth rate (darker regions).

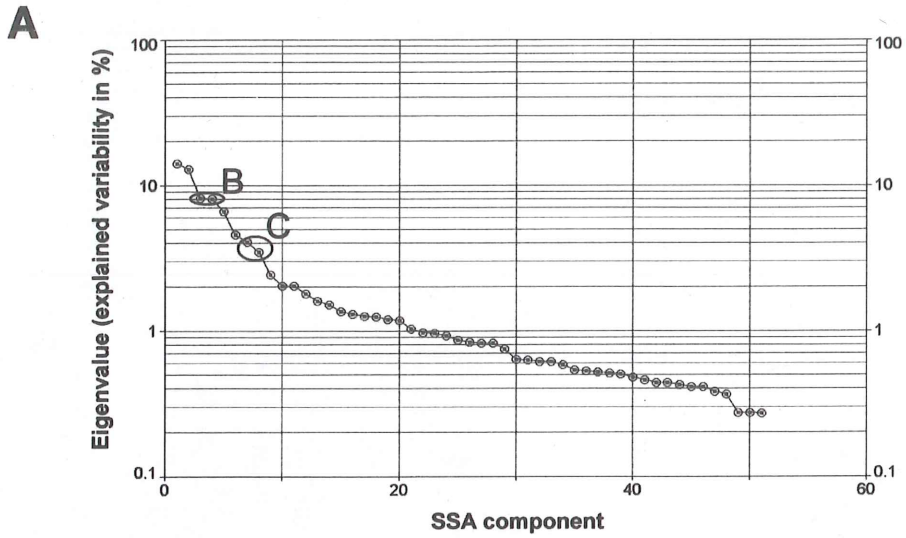

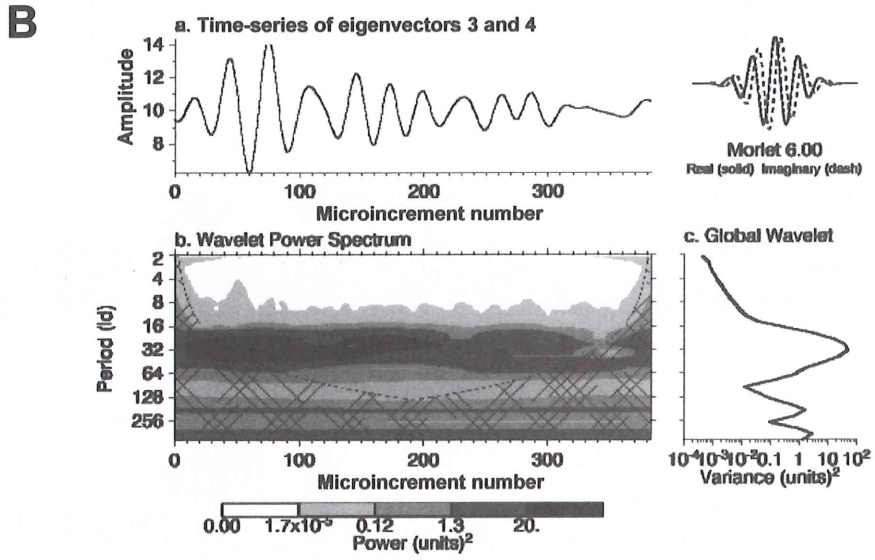

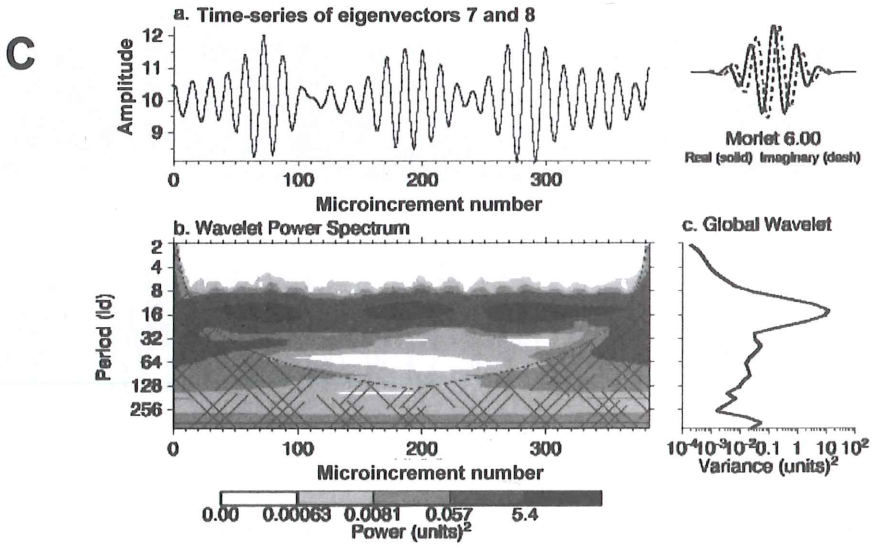

Plate 5. A–C. Single spectrum analysis (eigenvalue decomposition) of specimen 1 (A) and continuous wavelet transforms of selected eigenvalues (B, C). Eigenvalues 3 and 4 explain about 16% (A; 8% and 8%) of the chronology and resemble microincrement width periods of ca. 15 laminae (B), whereas eigenvalues 7 and 8 stand for periods of ca. 30 microincrements (C) and explain 4% and 3% of the time-series, respectively. These periods are interpreted as reflecting fortnightly periodicity of belemnite growth.

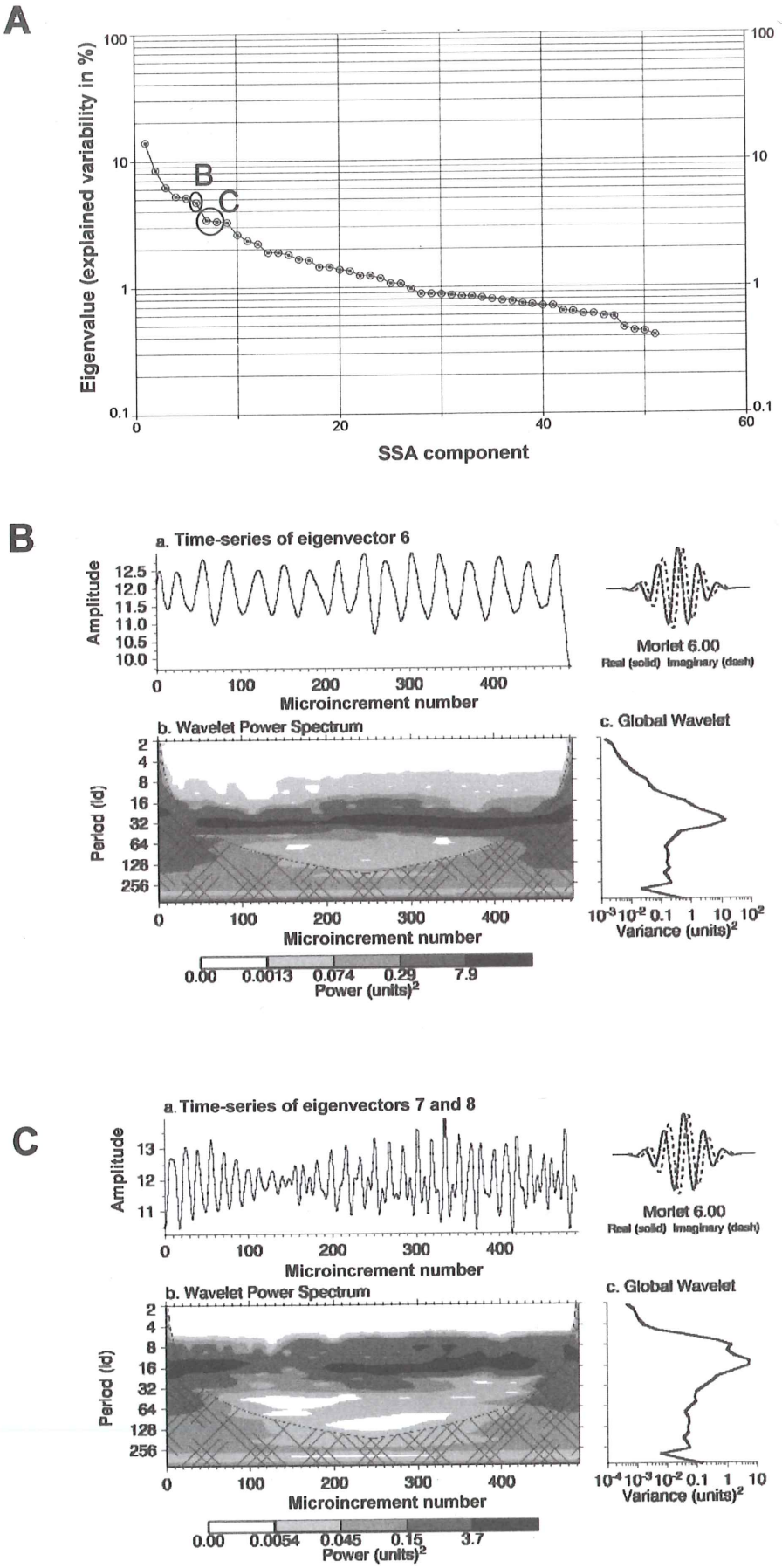

Plate 6. A–C. Single spectrum analysis (eigenvalue decomposition) of specimen 7 (A) and continuous wavelet transforms of selected eigenvalues (B, C). Eigenvalue 6 explains about 5% (A) of the chronology and resemble microincrement width periods of ca. 15 laminae (B), whereas eigenvalues 7 and 8 stand for periods of ca. 30 microincrements (C) and explain 7% (ca. 3.5% and 3.5%, respectively) of the time-series. These periods are interpreted as reflecting fortnightly periodicity of belemnite growth.